



A MODEL TEST AND ANALYSIS ON SEISMIC RESPONSE CONTROL OF BRIDGES BY MR-DAMPERS

Kazuhiko KAWASHIMA¹, Goh NAKAMURA², and Anat RUANGRASSAMEE³

SUMMARY

This paper presents a seismic response analysis of a standard viaduct to show the effectiveness of the variable dampers in reducing the deck displacement under a strong ground motion. Since a magnetorheological damper (MR-dampers) is effective as a variable damper, its application to the variable damper was studied by a cyclic loading test. A shaking table test was also conducted to clarify the effectiveness of the MR-damper as the variable damper.

INTRODUCTION

Seismic isolation has been extensively used for construction of highway bridges in Japan since the 1995 Kobe earthquake. In the seismic isolation, a lateral deck displacement of a standard viaduct often exceeds +/- 0.5m under a near-field ground motion. It is required in the seismic isolation not to constrain the deck response displacement so that the energy dissipation by isolators can be activated. As a consequence, a large clearance (gap) is required between adjacent decks for not having poundings between the decks. However this requires expansion joints which accommodate with large gap. Large expansion joints increase noise and vibration pollution due to the traffic load, resulting in a maintenance problem, as well as cost increase.

Consequently, it is required to decrease the lateral deck displacement of an isolated bridge without diminishing the effectiveness of seismic isolation. If supplemental dampers are provided between a deck and columns, energy dissipation increases. If the variable dampers which can vary damping forces depending on the bridge response are used, the seismic response of the bridge can be effectively controlled [1]. Kawashima and Unjoh developed a variable damper with the maximum damping force of 500kN using a standard viscous damper and a bi-path with a controllable orifice. By varying the section size of the orifice, they controlled the damping force. Recently the magnetorheological dampers (MR-dampers) were developed [2, 3], and it is shown that MR-dampers are effective in changing the damping force arbitrarily. It is expected to use MR-dampers as the variable dampers [4].

¹ Professor, Tokyo Institute of Technology, Tokyo, Japan. E-mail: kawashima@cv.titech.ac.jp

² Graduate Student, Tokyo Institute of Technology, Tokyo, Japan, gohgoh@cv.titech.ac.jp

³ Lecturer, Chulalongkorn University, Bangkok, Thailand. E-mail: fcearr@eng.chula.ac.th

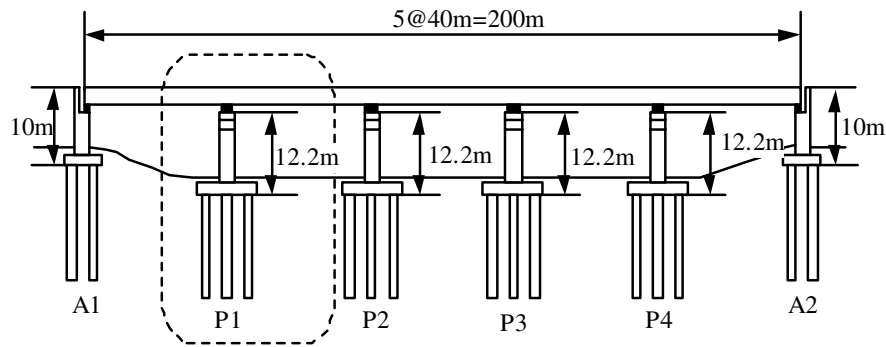


Fig. 1 Target Bridge

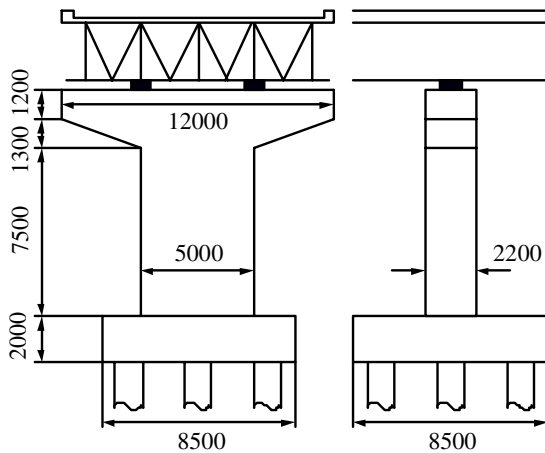


Fig. 2 Target Bridge

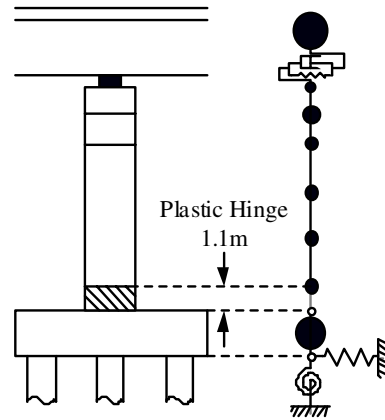


Fig. 3 Analytical Model

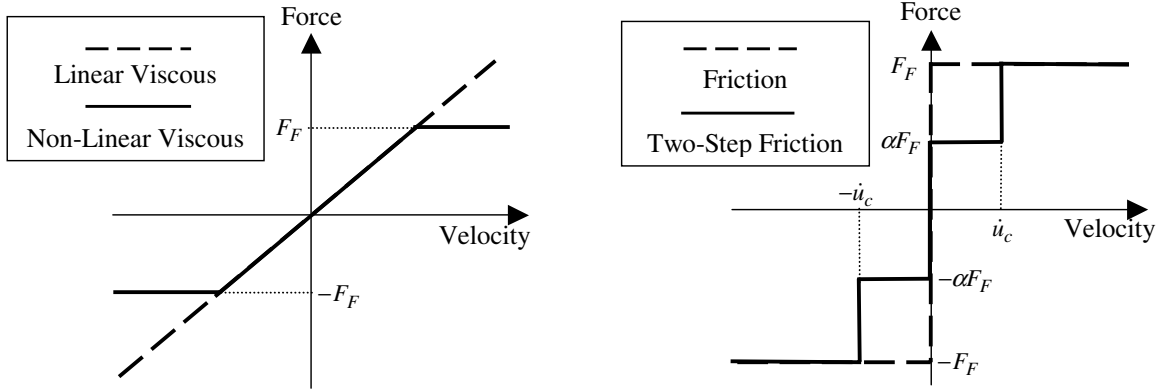
Based on such a background, a numerical analysis for seismic response of a 10m tall standard viaduct is first presented here to show the effect of four control algorithms. Then, a cyclic loading test of a MR damper and a shaking table test of a model bridge with the MR-damper are presented to show the applicability of a MR-damper to a variable damper.

EFFECTIVENESS OF VARIABLE DAMPERS

Target Bridge and Analytical Idealization

Fig.1 shows a target bridge consisting of a 5-span continuous deck supported by reinforced concrete columns and pile foundations. The bridge was designed in accordance with the Japanese post Kobe earthquake design code. Each span is 40 m long and 12 m wide. Since the geometric condition is nearly the same along the bridge axis, only a column (P1) with the tributary mass (6.96MN) is analyzed here as shown in Fig. 2. The deck is supported by two 80 mm-thick 900 mm by 900 mm elastomeric isolators with a lateral stiffness of 9.9 MN/m. The fundamental natural period of the bridge system consisting of the deck, the elastomeric isolators, the column and the pile foundation is 1.3 s. A variable damper is set between the deck and the column.

The target bridge is idealized by a 2 dimensional discrete model as shown in Fig.3. Response in the longitudinal direction is analyzed here because it is the major concern in seismic design. The flexural



(a) Viscous and Non-Linear Viscous Controls

(b) Friction and Two-Step Friction Controls

Fig. 4 Damping Force Schemes

hysteretic behavior of the column at the plastic hinge region was idealized by the Takeda degrading model [6]. By disregarding the crack point, it was simplified to a bilinear degrading model assuming the yield stiffness as the initial stiffness. N-S component measured at JMA Kobe Observatory during the 1995 Kobe earthquake is used as an input ground motion.

Control Algorithms

Four damping force algorithms are used for the variable dampers in dynamic response analyses [2, 3, 7], (1) viscous, (2) non-linear viscous, (3) friction and (4) two-step friction. They are represented as follows;

$$\underline{\text{Viscous}} \quad F_D = c\dot{u} \quad (1)$$

$$\underline{\text{Nonlinear Viscous}} \quad F_D = c\dot{u} \leq D_{Dy} \quad (2)$$

$$\underline{\text{Friction}} \quad F_D = \begin{cases} F_F & \cdots \quad \dot{u} > 0 \\ -F_F & \cdots \quad \dot{u} < 0 \end{cases} \quad (3)$$

$$\underline{\text{Two-Step Friction}} \quad F_D = \begin{cases} F_F & \cdots \quad \dot{u} > \dot{u}_c \\ \alpha F_F & \cdots \quad 0 < \dot{u} \leq \dot{u}_c \\ -\alpha F_F & \cdots \quad -\dot{u}_c \leq \dot{u} < 0 \\ -F_F & \cdots \quad \dot{u} < -\dot{u}_c \end{cases} \quad (4)$$

in which F_D : damping force, u and \dot{u} : relative displacement and velocity between the deck and the column, c : viscous coefficient, F_{Dy} : yield damping force, F_F : friction force, α : coefficient to represent the intensity of friction force at 2nd step, and \dot{u}_c : threshold velocity.

Although a variable damper is not needed to produce a standard viscous damping force, it is included in the analysis as a reference response. The nonlinear viscous control is effective in reducing the hysteretic behavior of the column. The limited maximum damping force prevents a build up of the plastic deformation of the column at the plastic hinge region.

On the other hand, although the friction control is effective in dissipating energy associated with relative displacement u between the deck and the column, the deck is locked to the column at low velocity \dot{u} if

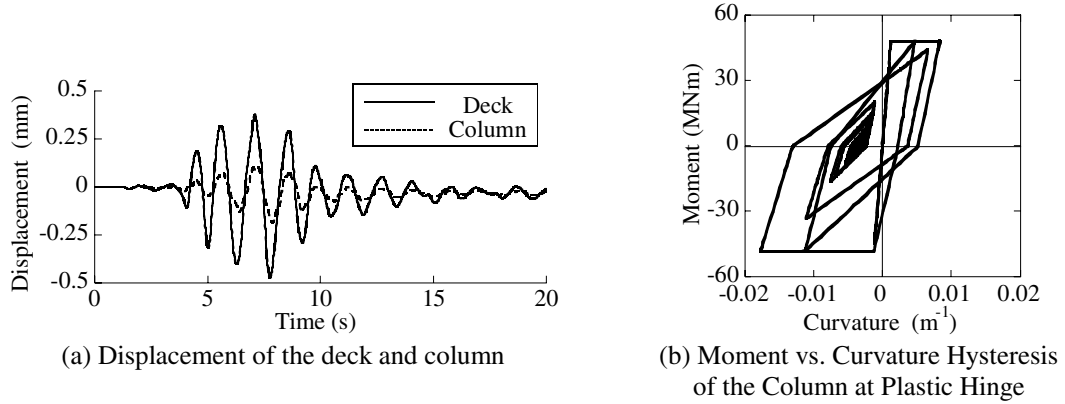


Fig.5 Seismic Response of the Bridge without Dampers

the damping force F_F is set high. The 2 step friction force \dot{u}_c control was developed to mitigate such a lock of the friction damper [2, 3]. By reducing the damping force from the original F_F to α times F_F at velocity \dot{u} smaller than \dot{u}_c , the lock can be avoided. The coefficient α and the threshold velocity \dot{u}_c have to be properly selected based on the response of bridge. It should be noted that although the damping force is controlled in 2 steps here for simplicity, it is possible to control it in arbitrary steps.

In the following analysis, c and F_{Dy} are assumed as 3.92 MN/m and 2.94 MN , respectively, under the viscous and nonlinear viscous controls. On the other hand, F_F , α and \dot{u}_c are assumed as 3.92 MN , 0.4 and 0.75 m/s , respectively, under the friction and 2 step friction controls.

Dynamic Response of the Target Bridge

Fig.5 shows the responses of the original bridge without setting the variable damper. The maximum displacements of deck and column are 0.469 m and 0.182 m , respectively. It is noted that since gap between decks is usually in the range of $150\text{-}200 \text{ mm}$, this deck displacement is excessive, which results in poundings between the decks. The column yields at the plastic hinge with the curvature ductility factor of 14.4.

Fig.6 shows the responses of the bridge with a variable damper under the viscous and the nonlinear viscous controls. Under the viscous control, the maximum deck displacement and the column curvature ductility factor reduces to 0.182 m and 3.2 , respectively. They are 39% and 22% of the responses of the bridge without the variable damper. The effect of the damper is significant to reduce the column plastic deformation. Although the deck displacement of 0.182 m is still large, pounding force may not be extensive no matter how poundings occur under this condition. The maximum damping force is 4.57 MN , which is 66% of the tributary weight of the deck.

On the other hand, the damping force does not build up larger than $F_{Dy} = 2.94 \text{ MN}$ under the nonlinear viscous control. Consequently, the maximum damping force under the nonlinear viscous control is 64% of that under the viscous control. The maximum deck displacement and the column curvature ductility factor are 0.21 m and 1.5 , respectively. The deck displacement increases by 16% compared to the response under the viscous control. This is due to the smaller damping force in the nonlinear viscous control. However the smaller damping force results in 53% smaller column curvature ductility factor of 1.5 than that under the viscous control. Thus, the smaller hysteretic response in the column can be realized by the smaller damping force in the nonlinear viscous control.

The energy dissipated in the column at the plastic hinge E_C and the variable damper E_D may be written as

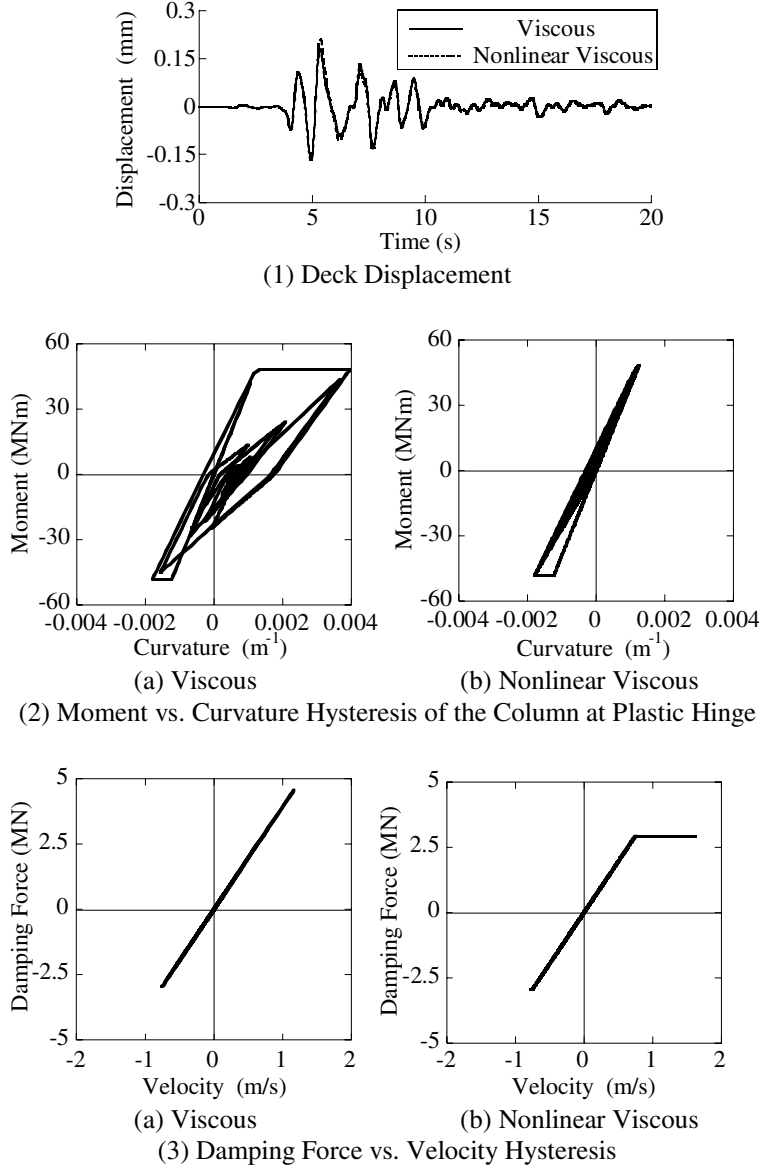


Fig.6 Seismic Response of the Bridge under Viscous and Nonlinear Viscous Controls

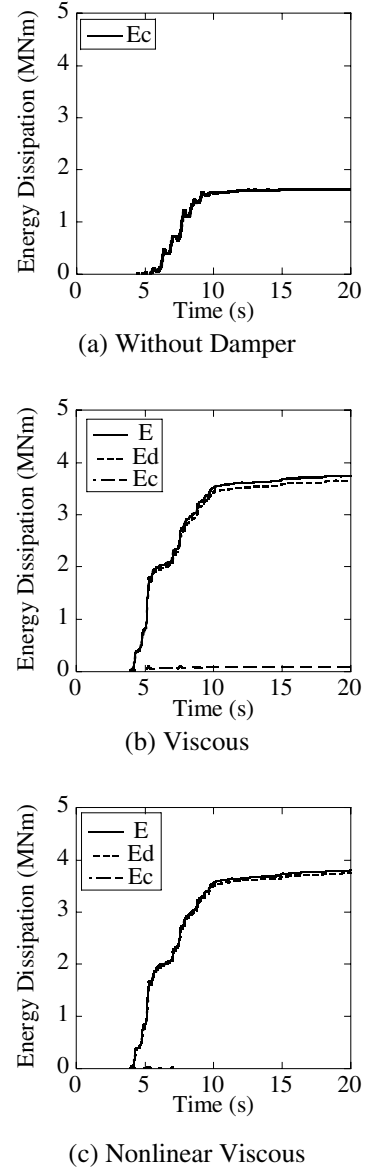


Fig.7 Energy Dissipation of the Bridge under Viscous and Nonlinear Viscous Controls

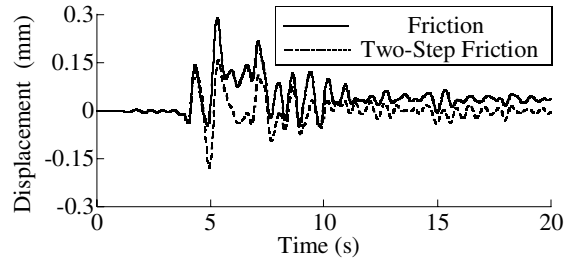
$$E_c = L_p \cdot \int M \cdot \dot{\phi} \cdot dt \quad (5)$$

$$E_D = \int F_D \cdot \dot{u} \cdot dt \quad (6)$$

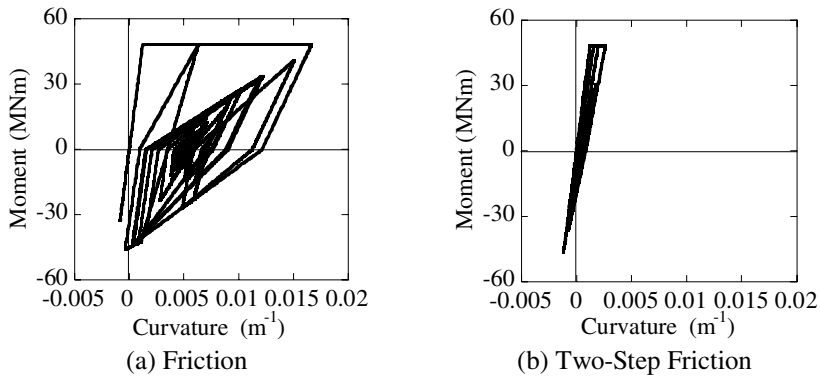
$$E = E_c + E_D \quad (7)$$

in which L_p : plastic hinge length, M : moment at the plastic hinge, $\dot{\phi}$: curvature velocity at the plastic hinge, F_D and \dot{u} : damping force and velocity of the variable damper, respectively, and E : sum of the energy dissipation in the column at the plastic hinge and the variable damper.

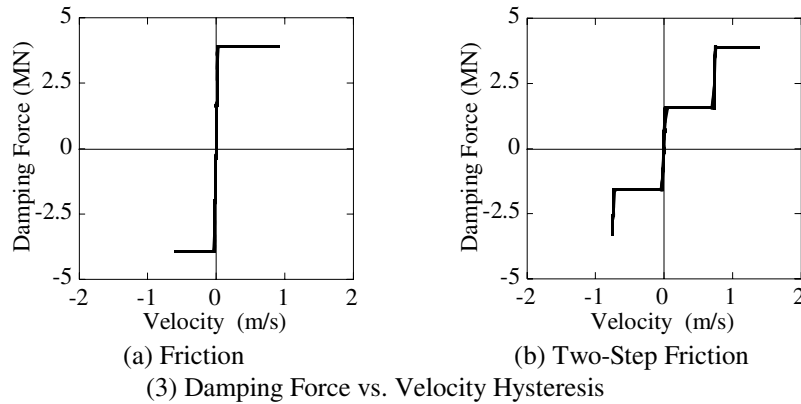
Fig. 7 compares E_c , E_D and E . The energy dissipated at the column E_c is $1.63MNm$ in the bridge without the damper, while it is nearly zero under the viscous and nonlinear viscous controls. The energy dissipation by the variable damper E_D under the nonlinear viscous control is about the same with that



(1) Deck Displacement



(2) Moment vs. Curvature Hysteresis of the Column at Plastic Hinge



(3) Damping Force vs. Velocity Hysteresis

Fig.8 Seismic Response of the Bridge under Friction the Two-Step Friction Controls

under the viscous control. In spite of smaller damping force, almost the same amount of energy is dissipated due to larger relative displacement between the deck and the column under the nonlinear viscous control.

The bridge response with a variable damper under the friction and the two-step friction controls is shown in Fig.8. The maximum deck displacement and the column curvature ductility factor are 0.287 m and 13.6, respectively, under the friction control. They are 61% and 94% of the responses without the variable damper, respectively. The deck displacement substantially decreases by providing the damper under the friction control. However the hysteretic response of the column at the plastic hinge is nearly the same to the response without control. This is because the deck is “locked” to the column as shown in Fig. 9. As a consequence, the energy dissipation by the variable damper E_D is only 1.53MNm as shown in Fig. 10.

On the other hand, the effect of 2 step friction control is obvious to mitigate the hysteretic response of the column at the plastic hinge. The column curvature ductility factor and the deck displacement are only 2.1 and 0.174 m, respectively, which are only 15% and 61 % of those under the friction control. Two and a

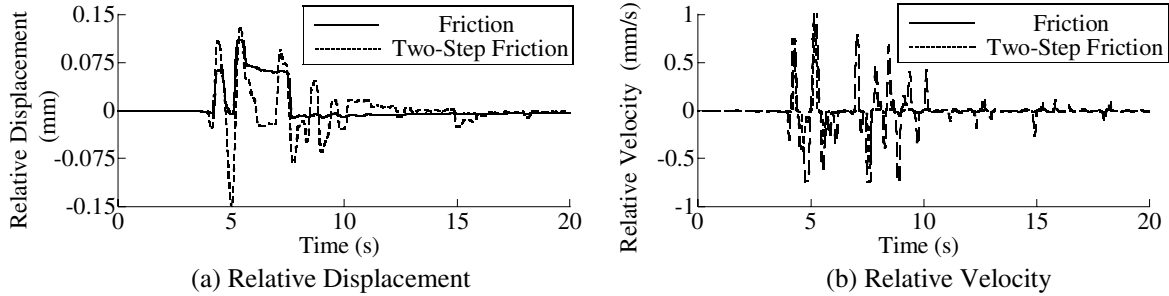


Fig.9 Relative Displacement and Velocity between the Deck and Column

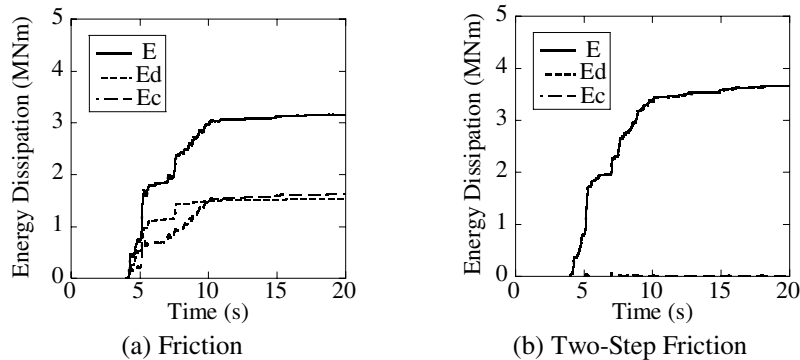


Fig.10 Energy Dissipation of the Bridge under Friction and Two-Step Friction Controls

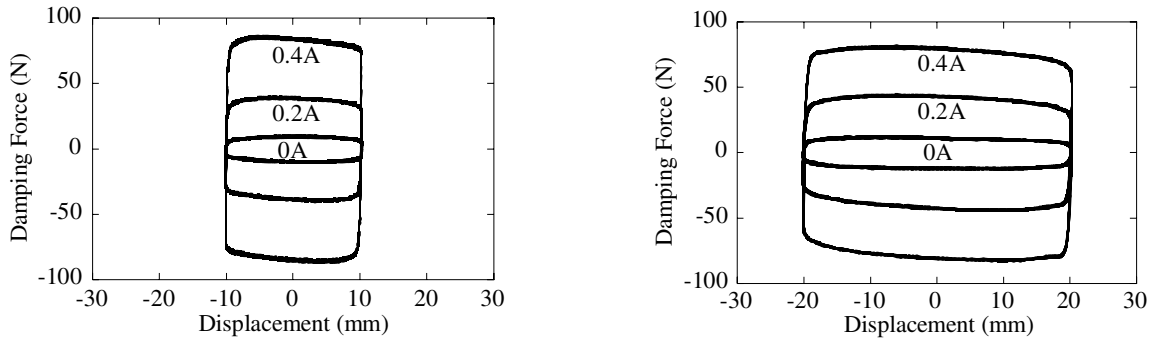


Fig.11 Damping Force Hystereses of the MR-Damper

half times larger energy dissipation by the variable damper under the 2 step friction control brings the smaller column ductility factor and deck displacement.

CYCLIC LOADING TEST OF A MR-DAMPER

Determination of Parameters

To study the applicability of MR-dampers to the variable dampers, the performance of a MR-damper was clarified to a Lord Corporation MR-damper with 100N capacity (RD1084-1B) and a current driver (RD3002) system. The MR-damper was cyclically loaded by an actuator under displacement control by varying amplitude and frequency. Fig. 11 shows the damping force F_D vs. displacement u hystereses at frequency of 0.5 and 2.5 Hz. Nearly rectangular hystereses are produced by the MR-damper under constant currents. Fig. 12 shows a frequency dependence of damping force F_D . Since the frequency

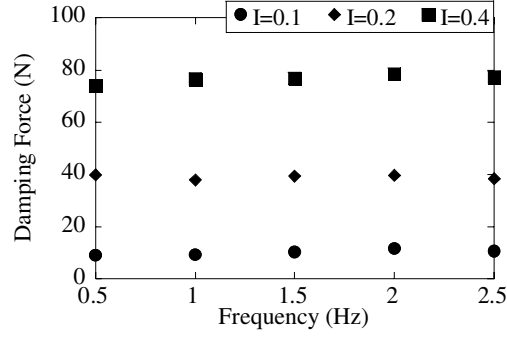


Fig.12 Dependence of the Damping Force on Loading Frequency

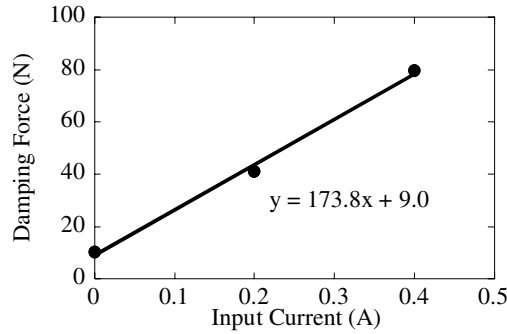
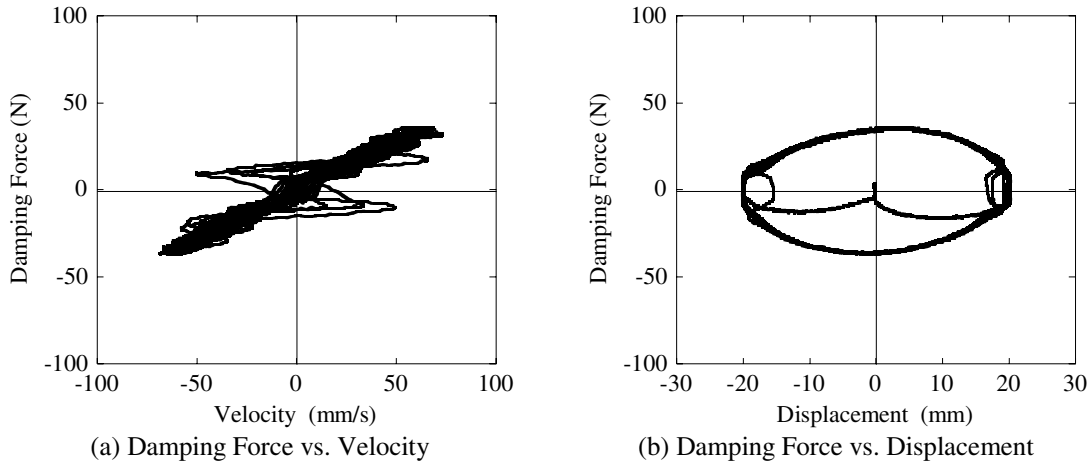


Fig. 13 Damping Force vs. Current Relation



(a) Damping Force vs. Velocity

(b) Damping Force vs. Displacement

Fig. 14 Hystereses of Damping Force under the Viscous Control

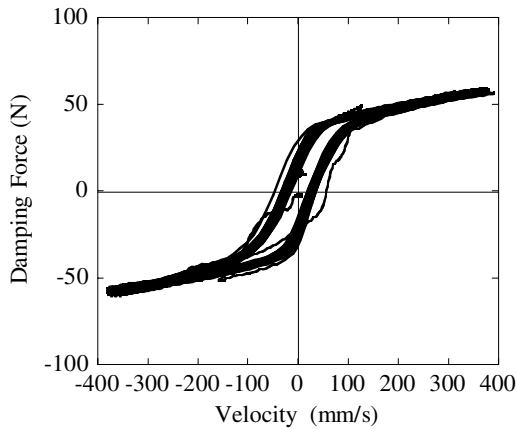
dependence of damping force F_D is less significant, the damping force F_D vs. current I relation is obtained as shown in Fig. 13. This relation may be represented as

$$F_D = 173.8I + 9.0 \quad (8)$$

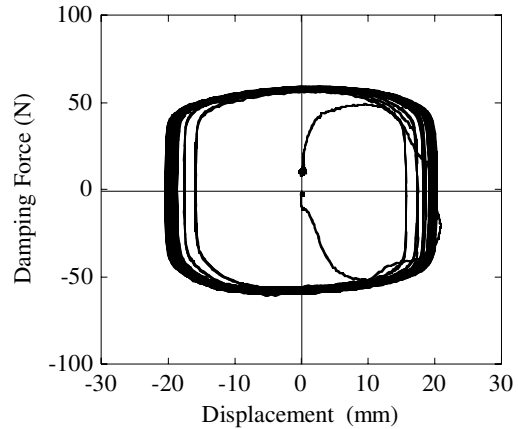
The second term represents a friction between a piston and a cylinder of the MR-damper.

Control Algorithm

The MR-damper was controlled by the viscous, the nonlinear viscous, the friction and the 2 step friction algorithms represented by Eqs. (1)-(4), respectively. The damping force was controlled by current using Eq. (8). Figs. 14 and 15 show F_D vs. u and F_D vs. \dot{u} hystereses of the MR-damper under the viscous and



(a) Damping Force vs. Velocity



(b) Damping Force vs. Displacement

Fig. 15 Hystereses of Damping Force under the Nonlinear Viscous Control

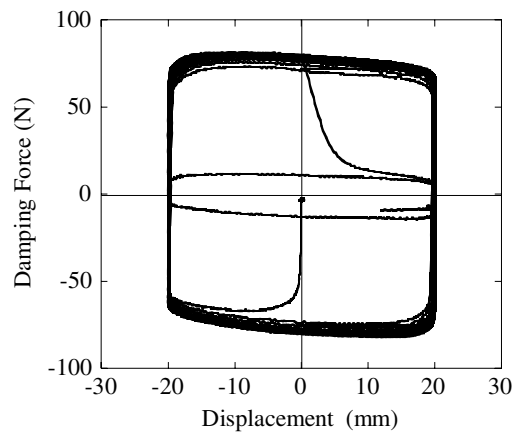
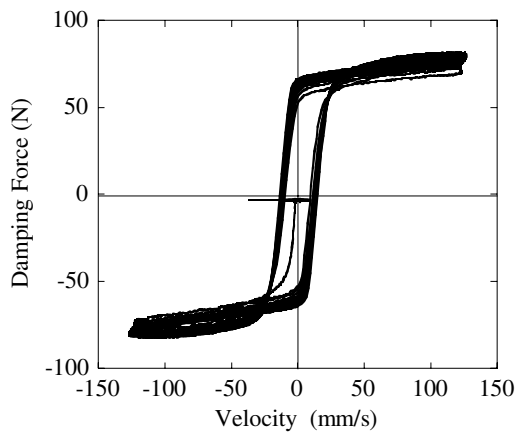
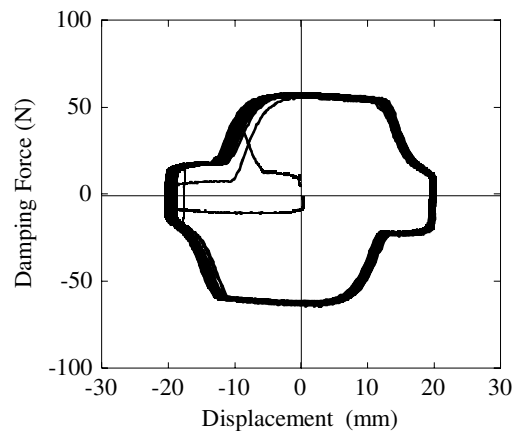
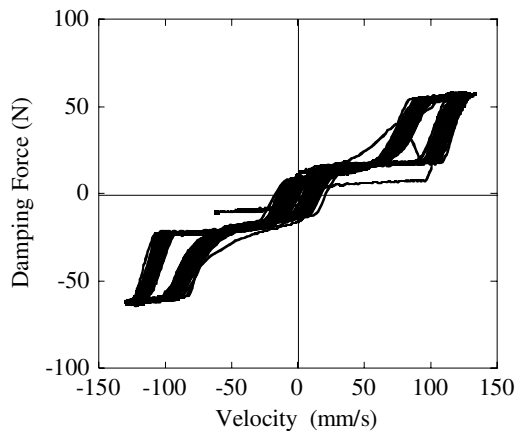


Fig. 16 Hystereses of Damping Force under the Friction Control



(a) Damping Force vs. Velocity

(b) Damping Force vs. Displacement

Fig. 17 Hystereses of Damping Force under the Viscous Control

the nonlinear viscous controls. F_{Dy} was set 80 N in the nonlinear viscous control. Overall behavior of the MR damper is close to the expected hystereses under the viscous control, however a certain error occurs at small velocity where sign of the damping force changes. Sharpe change of damping force prevents to

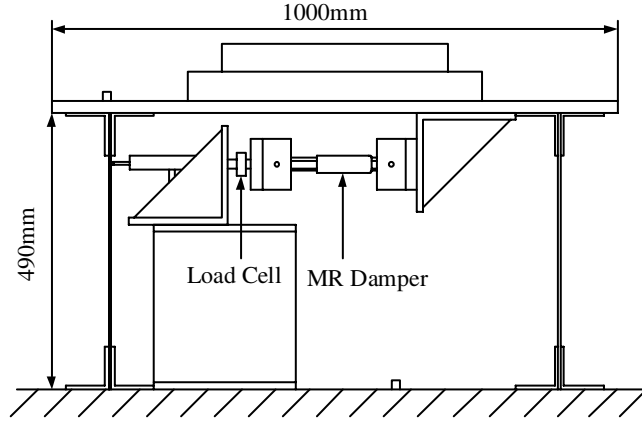


Fig. 18 Model Bridge for Shaking Table Test

produce smooth ellipsis variation of the damping force near zero velocity. On the other hand, the damping force does not reach 80 N under the nonlinear control although it continues to increase at $|\dot{u}| \leq 150\text{ mm/s}$. Furthermore loading and unloading paths are not identical at $|\dot{u}| \leq 100\text{ mm/s}$. This results from the time delay of the MR-damper inherent to time required for MR fluid to respond a command.

Figs. 16 and 17 show F_D vs. u and F_D vs. \dot{u} hystereses of the MR-damper under the friction and the 2 step friction controls. The damping force F_F in Eq. (3) was set 79 N under the friction control, and F_F and the parameter α in Eq. (4) were set 60 N and 0.25 , respectively, in the 2 step friction control. Damping forces produced by the MR-damper under the friction control are close to the target damping forces except that the damping force slightly decreases as displacement increases. The time delay of MR-damper induces a smooth change of the damping force under the 2 step friction control.

It is found from the above tests that expected damping force can be approximately reproduced by the MR-damper using Eq. (8). However the time delay of the response of MR-damper results in some errors in reproducing damping force at higher loading rate.

SHAKING TABLE TEST

Model Bridge and Shaking Table Test

A shaking table test of a model bridge with a MR-damper was conducted to show the application of variable damper. The same MR-damper used in the cyclic loading test was used for the shaking table test. The model was made of steel, and it was 1 m long and 0.49 m high with a deck mass of 199 kg as shown in Fig. 18. Since the purpose of shaking table test is to provide an experimental data set which can be used to verify an analytical model, a special attention was not paid to follow the similarity law. It is very limited to produce a small scaled-model. The flexural stiffness of the steel columns was so determined that the fundamental natural period of the model becomes 0.47 s . Damping ratio of the model without setting the MR-damper is 2.7% by free oscillation decays.

The JMA Kobe ground motion presented in the previous section was used as an input table motion by scaling down the peak ground acceleration. Viscous coefficient c , the yield viscous damping force F_{Dy} , the friction force F_F and the coefficient α in Eqs. (1)-(4) were set 1.0 Ns/mm , 30 N , 80 N and 0.25 , respectively.

Fig. 19 shows deck displacements of the model without the MR-damper. Computed responses which will be described later are presented here for comparison. As shown in Table 1, peak deck displacement is 10.4 mm and 25.2 mm at the peak table acceleration of 0.086 g and 0.196 g , respectively.

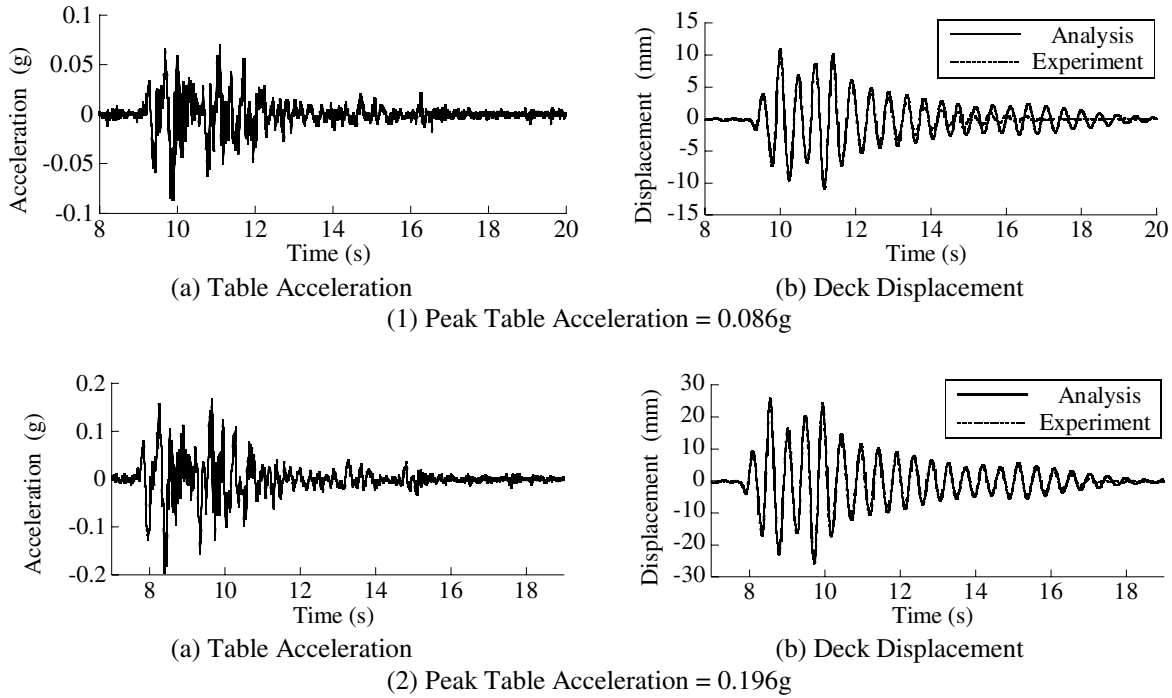


Fig. 19 Seismic Response of Model Bridge without Damper

Table. 1 Summary of Shaking Table Tests

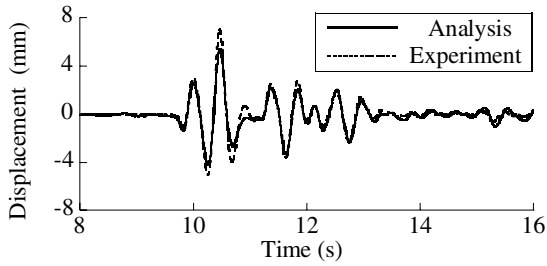
Control	Table acceleration (g)	Deck displacement (mm)	Damping force (N)
Without damper	0.086	10.4	-
	0.196	25.2	-
Viscous	0.088	7.1	60.8
Nonlinear viscous	0.092	7.6	26.7
Friction	0.182	16.3	75.6
2 step friction	0.192	19.7	68.2

Figs. 20 and 21 show deck displacements and damping forces of the model with the MR-damper under viscous and nonlinear viscous controls, respectively. Similar to Fig. 19, an analytical simulation which will be described later is presented here for comparison. In the viscous control, a rate of velocity dependence of the damping force (viscous coefficient) is higher than expected at the velocity lower than about 10 mm/s, while it is lower than expected at the velocity higher than 10 mm/s. Because of F_{Dy} , such a variation of the viscous coefficient is not apparent, but undershooting of the damping force is significant under the nonlinear viscous coefficient.

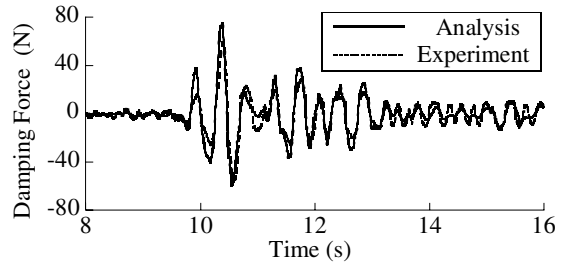
Figs. 22 and 23 show the response of the model bridge with the MR-damper under friction and 2 step friction controls, respectively. Similar trend is observed in those results.

Analytical Simulation

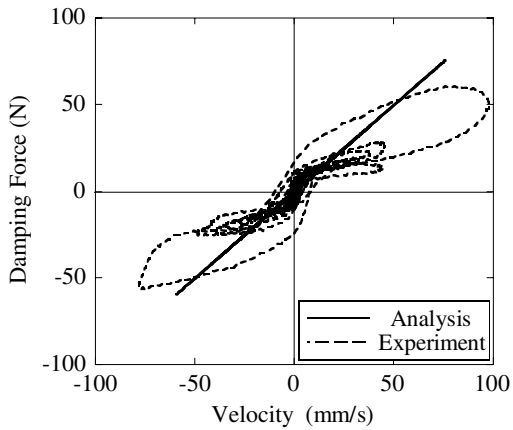
The model bridge was idealized by a discrete analytical model as shown in Fig. 24. The analytical model was formed based on the measured section properties. Only the column stiffness was slightly modified so that the fundamental natural period of the analytical model becomes 0.47 s, which was measured in the free oscillation test. Damping force was idealized by the Rayleigh damping, and 2 parameters of the



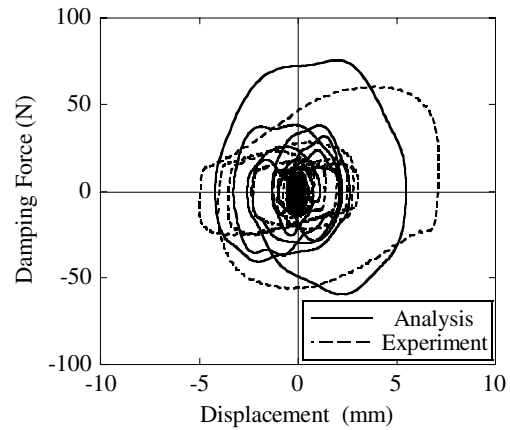
(a) Deck Displacement



(b) Damper Force

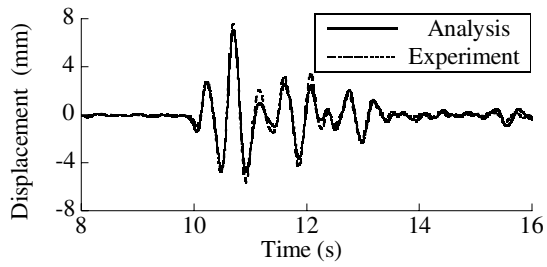


(c) Damping Force vs. Velocity Hysteresis

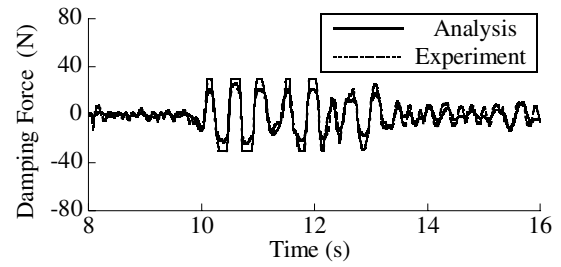


(d) Damping Force vs. Displacement Hysteresis

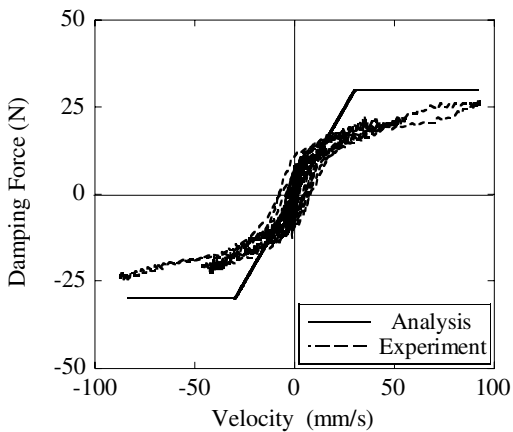
Fig. 20 Seismic Response of Model Bridge with a MR-damper under Viscous Control



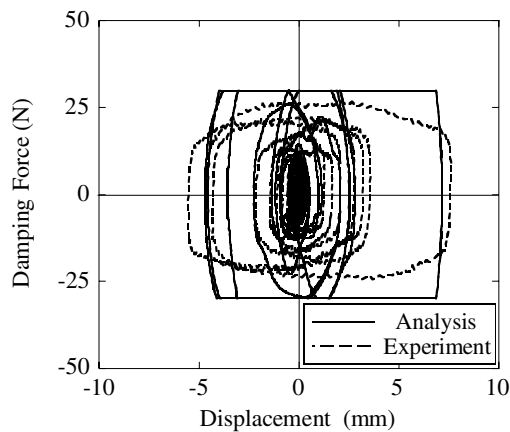
(a) Deck Displacement



(b) Damper Force

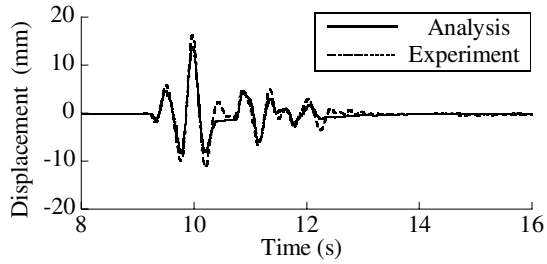


(c) Damping Force vs. Velocity Hysteresis

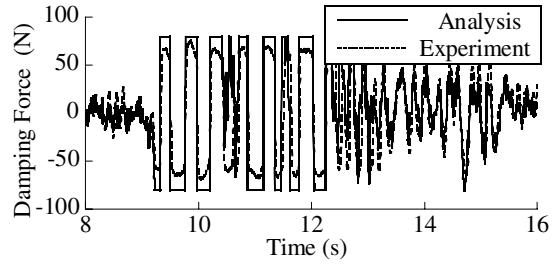


(d) Damping Force vs. Displacement Hysteresis

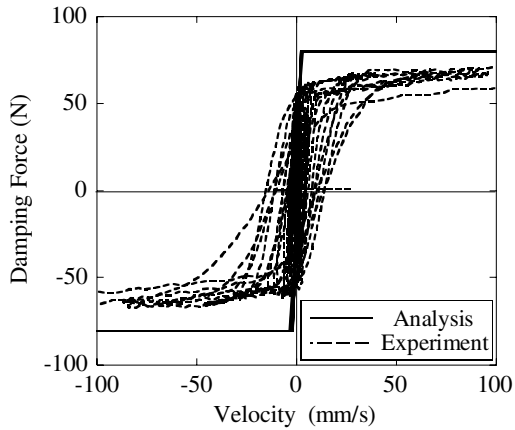
Fig. 21 Seismic Response of Model Bridge with a MR-damper under Nonlinear Viscous Control



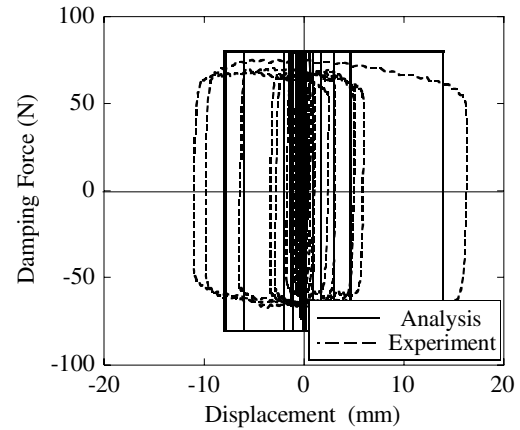
(a) Deck Displacement



(b) Damper Force

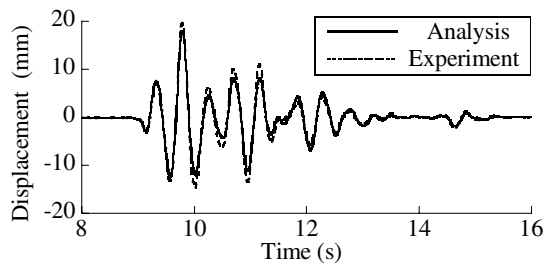


(c) Damping Force vs. Velocity Hysteresis

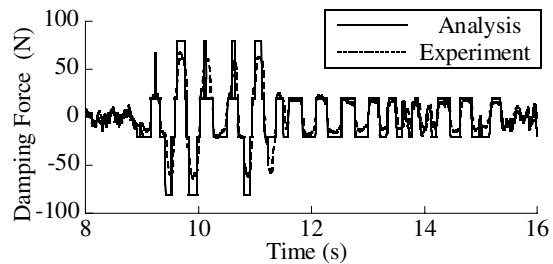


(d) Damping Force vs. Displacement Hysteresis

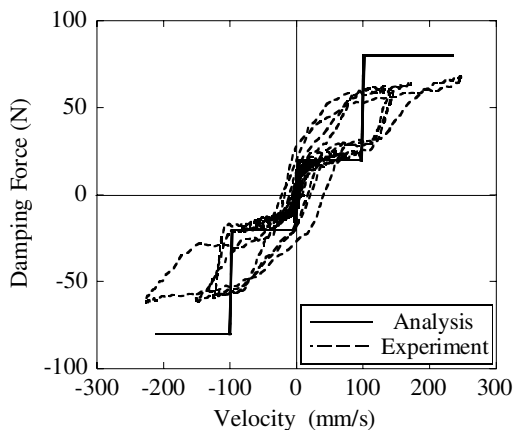
Fig. 22 Seismic Response of Model Bridge with a MR-damper under Friction Control



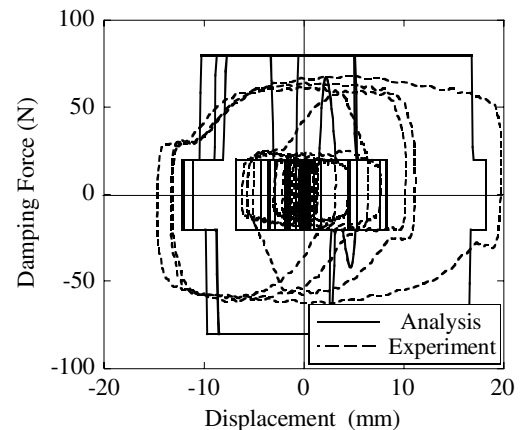
(a) Deck Displacement



(b) Damper Force



(c) Damping Force vs. Velocity Hysteresis



(d) Damping Force vs. Displacement Hysteresis

Fig. 23 Seismic Response of Model Bridge with a MR-damper under 2 Step Friction Control

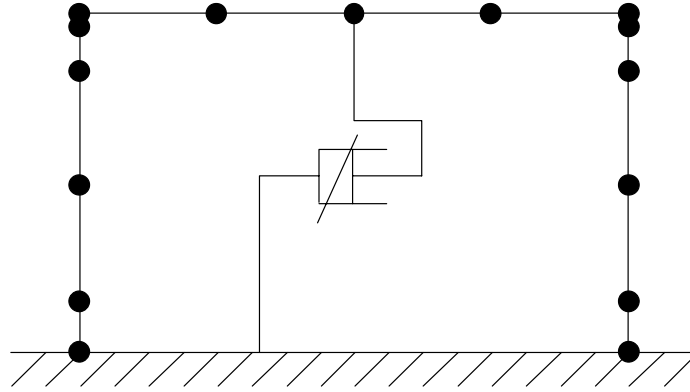


Fig. 24 Analytical Model of Model Bridge

Rayleigh damping force were determined so that the 1st and 2nd modal damping ratios become 0.027, which was measured in the free oscillation decay of the model. The MR-damper was idealized by a nonlinear damper element.

Computed responses are presented in Figs. 20-23. The computed responses of the model without the MR-damper are very close to the measured responses. The deck displacements are well correlated by the analysis under the viscous, nonlinear viscous, friction and 2 step friction controls, in spite of the error in producing the expected damping forces in the model bridge. Correlation for the damping forces should be re-clarified after improving the control of MR-damper.

CONCLUSIONS

Seismic response analysis of a standard viaduct was conducted to show the effectiveness of variable dampers in the mitigation of deck displacement. An application of a MR-damper to the variable damper was clarified by a cyclic loading test and a shaking table test. A numerical correlation for the shaking table test was conducted. From the results presented herein, the following conclusions may be deduced:

1. Compared to the viscous control, the column ductility factor reduces by 53% under the nonlinear viscous control because of the limited damping force. However, the deck displacement under the nonlinear viscous control increases by 16% compared to the viscous control due to less energy dissipation in the variable damper.
2. Although the friction damping control is effective in dissipating energy, “lock” occurs between the deck and the column at high damping force. The lock prevents energy dissipation to occur in the variable damper, which results in larger hysteretic deformation in the column at the plastic hinge. The 2 step friction control is effective in mitigating the lock. As a consequence, the 2 step friction control reduces the deck displacement and column ductility factor by 61% and 15%, respectively, compared to the responses under the friction control.
3. MR-dampers are effective as the variable dampers. The MR-damper used in this study can produce the target damping force by controlling current. However time delay of the response of MR-damper results in error in changing damping force at high velocity. This develops delay of reaching the damping force to an expected level or undershooting. Control algorithm has to be improved to mitigate this effect.
4. An analytical model which was formed based on the section properties well correlates the responses of shaking table test. However accuracy is limited when error of the produced damping force becomes significant due to the delay of the response of MR-damper.

REFERENCES

1. Kawashima, K. and Unjoh, S. "Seismic response control of bridges by variable dampers." *Journal of Structural Engineering*, ASCE, 1994: 120-9, 2584-2602
2. Ruangrassamee, A. and Kawashima, K. "Experimental study on semi-active control of bridges with use of magnetorheological damper." *Journal of Structural Engineers*, JSCE, 2001: 47A, 639-650
3. Ruangrassamee, A. and Kawashima, K. "Control of bridge response with pounding effect by variable dampers." *Engineering Structures*, 2003: 25-5, 593-606
4. Spencer, B., Dyke, S.J., Saint, M.K., and Carlson, J. "Phenomenological model of a magnetorheological damper." *Journal of Engineering Mechanics*, ASCE, 1997: 123-3, 230-238
5. Sunakoda, K., Sodeyama, H., Iwata, N., Fujitani, H. and Soda, S. "Dynamic characteristics of magnetorheological fluid damper." 7th SPIE Annual International Symposium on Smart Structures and Materials, Newport Beach, USA, 2000
6. Takeda, T., Sozen, M.A. and Nielsen, N.N. "Reinforced concrete response to simulated earthquakes." *Proc. 3rd Japan Earthquake Symposium*, 1970: 357-364
7. Nakamura, G., Ruangrassamee, A. and Kawashima, K. "Application of MR Dampers to Variable Dampers." *Proc. JSCE*, submitted for publication